

Phase segregation and impact toughness in linear low density polyethylene*

A. D. Channell, E. Q. Clutton and G. Capaccio†

BP Chemicals Research and Development Centre, PO Box 21, Grangemouth FK3 9XH, UK

The impact behaviour of three linear low density polyethylenes (LLDPE) has been studied using the energy partitioning methodology recently developed in this laboratory. The aim was to elucidate the origin of the high toughness of this class of polymers and to establish whether a rubber toughening mechanism is involved. It has been found that LLDPEs have an unexpectedly high intrinsic toughness, and that there is a significant ductile contribution to the total fracture energy from shear lip energy absorption. No evidence of a conventional rubber toughening mechanism has been found. However, the shear lip area (and hence this specific component of the total fracture energy) increases with the concentration of the segregated 'rubbery' phase.

(Keywords: impact toughness; phase segregation; LLDPE)

INTRODUCTION

The fracture behaviour of linear low density polyethylene (LLDPE) has been studied by several authors^{1,2}. Although the measurements vary in kind, consistently high values of toughness have been measured. Interestingly, these values are comparable to, or higher than, those measured for tough engineering polymers^{3,4} and considerably higher than those for high density polyethylene⁵. The high levels of toughness in LLDPE have been attributed to the morphology of the polymer, and in particular to the presence of discrete domains ($\sim 0.2 \mu\text{m}$ in diameter) of rubber-like material⁶. This is a characteristic feature of many LLDPEs which results from the segregation of highly branched non-crystallizable molecules⁷⁻⁹. Mirabella *et al.*⁶ proposed a rubber toughening mechanism to explain the performance of LLDPE.

In recent years, however, it has become apparent that the extent to which segregation occurs in LLDPE varies considerably from material to material. This would cast doubt upon the validity of any simple generalization. The development, in our laboratory, of a new methodology to investigate the impact response of materials^{5,10,11} and the availability of well characterized samples, provided the stimulus for a fresh appraisal of the mechanisms responsible for the toughness of LLDPE.

EXPERIMENTAL

Materials

The materials studied in this work had a density of 920 kg m^{-3} and a melt flow rate of 1.0 g per 10 min. Molecular weight distributions and crystallinities were determined by g.p.c. and d.s.c., respectively (Table 1).

* Presented at 'Polymer Science and Technology — a conference to mark the 65th birthday of Professor Ian Ward FRS', 21–23 April 1993, University of Leeds, UK

† To whom correspondence should be addressed

Transmission electron micrographs were taken of samples prepared using a modified Kanig technique¹². Blocks of the material were stained for 3 days prior to cutting sections using a Reichart and Jung Ultracut ultramicrotome, and the sections were then viewed using a Hitachi H600 transmission electron microscope.

The segregated 'rubbery' phase corresponds to the regions in Figure 1 which exhibit low stain uptake. The volume fraction of this phase was estimated from direct measurements on the micrographs.

Preparation of fracture specimens

Samples of each material were compression moulded¹³ into sheets $\sim 12 \text{ mm}$ thick. The required amount of polymer was pre-heated in the press for 30 min at 170°C . Slow cooling was then applied at 2°C min^{-1} . When the press was at 110°C , pressure was applied incrementally at each 5°C of cooling. At 80°C the samples were crash cooled.

Charpy impact specimens were made long enough to allow testing with an anvil span to specimen depth ratio of 6. Each specimen was notched mid-way along its length with a multi-toothed cutter; the notch depth to specimen depth ratio was 0.25. This ratio ensured that failure did not occur by plastic collapse¹¹.

Specimens (12 mm deep) for the measurement of initiation toughness had 0.5 mm deep side-grooves cut in

Table 1 Details of materials and samples used

	A	B	C
$M_w (\times 10^3)$	150	127	130
M_w/M_n	4.2	4.6	5.5
Crystallinity (%)	43.0	41.9	41.7
Volume fraction of segregated phase (%)	0	~ 1	~ 7.6
Yield stress (MPa)	25	21	25

M_w and M_n , weight- and number-average molecular weights, respectively

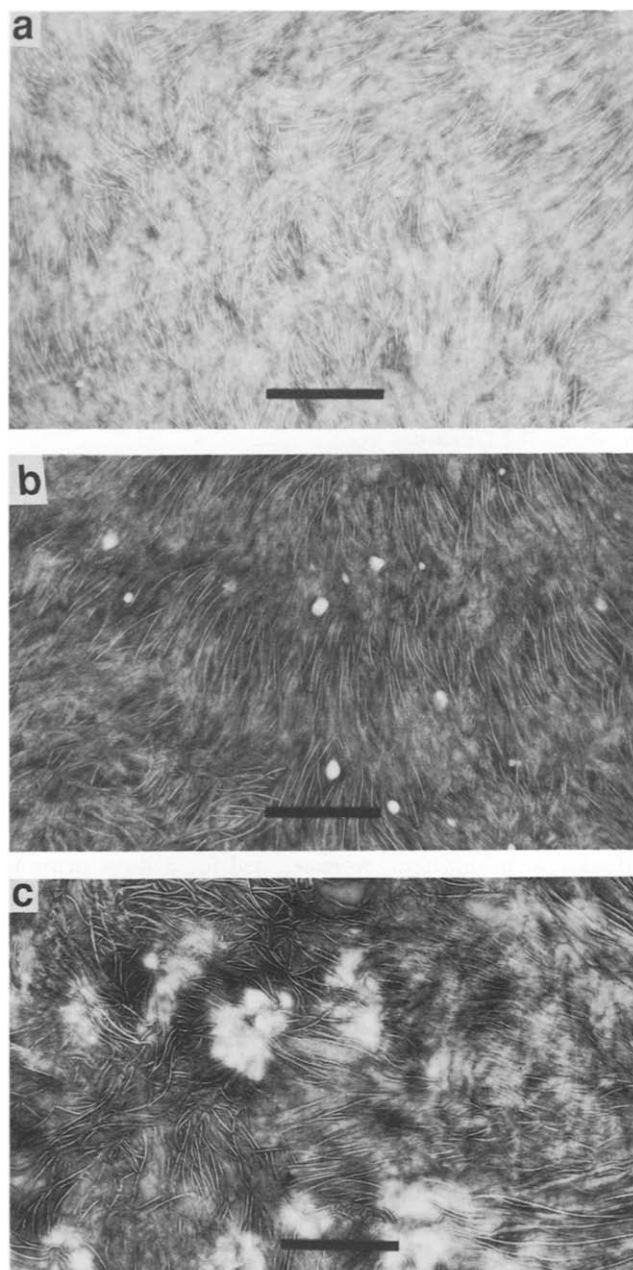


Figure 1 Transmission electron micrographs of sections of the three materials used: (a) A; (b) B; (c) C. Scale bar = 1 μm

the moulded surfaces. This was to eliminate any possible contribution due to shear lips.

For the detailed analysis of the energy associated with shear lips, 45° notches were machined at each corner and a razor notch was cut at the rear of the specimen. The former was to eliminate any effect due to the influence of the craze on shear lip formation (the depth of the corner notches was roughly equal to the craze length). The rear notch was to prevent the formation of a hinge at the back of the specimen: a blade was driven into the specimen to a depth equal to the hinge length (as observed in a conventional specimen). Different shear lip areas were obtained by varying specimen depth, i.e. 12, 18, 24 and 36 mm.

Impact testing

All impact testing was carried out at 0°C using a servo-hydraulic single stroke driven ram machine, with

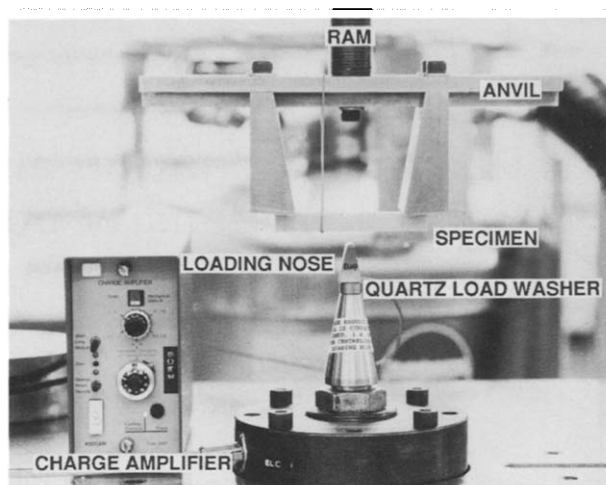


Figure 2 Experimental set-up

an inverted test geometry (Figure 2) to obtain the best signal to noise ratio. Loads were measured with a Kistler piezoelectric quartz load washer, the output of which was converted to a voltage by a charge amplifier, and recorded on a transient recorder prior to transfer to a computer for data analysis.

Toughness was determined using the method of Plati and Williams¹⁴, with the geometry specified above. Toughness, G , was defined by the equation:

$$G = \frac{U}{BD\phi} \quad (1)$$

where U is the measured energy, B is the specimen thickness, D the specimen depth, and ϕ the calibration factor which accounts for the change in compliance of the specimen due to the presence of a notch.

Impact tests were performed over a range of velocities. The limits on test velocity were determined by plastic collapse of the beams at low speed ($\sim 0.05 \text{ m s}^{-1}$) and the poor quality of the signal at high speeds ($\sim 3.0 \text{ m s}^{-1}$) due to dynamic effects.

RESULTS

Total toughness

Examination of the fracture surface (Figure 3a) reveals a number of features which characterize the failure phenomenon and which account for the energy absorbed. A craze zone is clearly visible which develops into the specimen depth from the root of the notch. Beyond it, there is a smooth area associated with brittle failure. Shear lips are detectable at the specimen surface. These are regions which have undergone a pronounced ductile deformation as a result of the biaxial stress field present at the free surface of the specimen. The crack arrests at the rear of the specimen with the formation of a hinge.

A typical force/deflection curve is shown in Figure 3b; the significance of the two distinct regions in these curves will be discussed in the following sections. Typical failure times were $> 1 \text{ m s}^{-1}$ and dynamic oscillations were negligible. Curves like the one shown in Figure 3b were recorded at different impact velocities and, from the integrated area, values of total toughness (G_t) were calculated using equation (1). The results are shown in Figure 4. Values of G_t at 1 m s^{-1} are also given in Table 2.

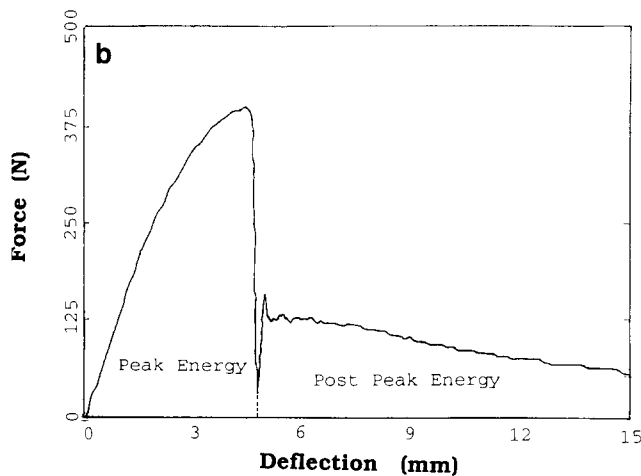
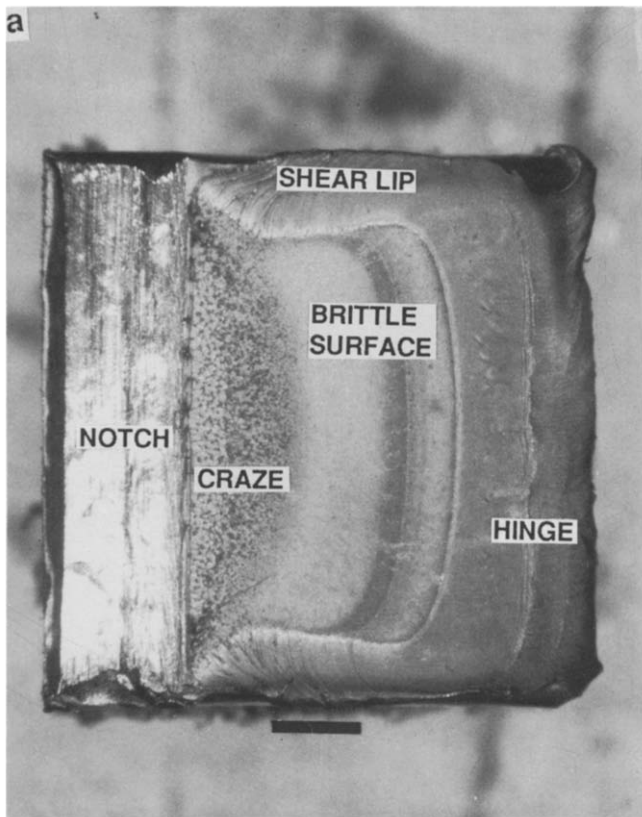


Figure 3 Determination of total toughness (G_t): (a) fracture surface (scale bar = 2 mm); (b) typical force/deflection curve

Table 2 Fracture toughness parameters measured at a velocity of 1 m s^{-1}

Material	G_t (kJ m^{-2})	G_p (kJ m^{-2})	G_{pp} (kJ m^{-2})
A	24	18	6
B	19	10	9
C	36	13	23

G_t values for the three materials fall approximately on three parallel bands. Material C, with the highest concentration of segregated phase, exhibits higher values of total toughness. The results for A and B, however, are not consistent with a simple correlation between G_t and the segregated phase. It is therefore instructive to pursue the analysis further and to probe the effect of the

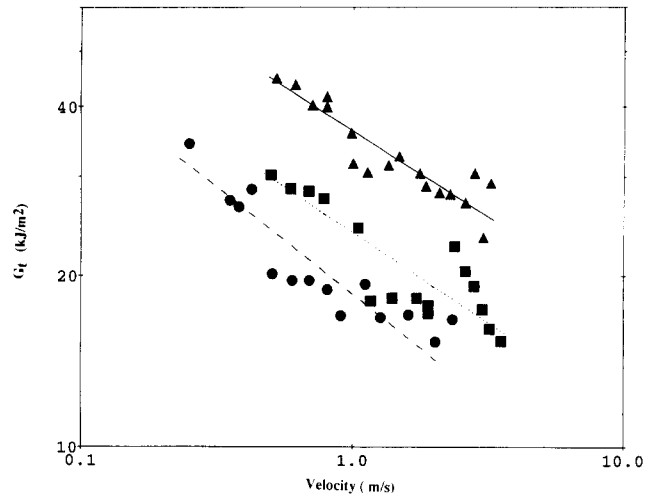


Figure 4 Total toughness (G_t) versus impact velocity: (■) A; (●) B; (▲) C

segregated phase on the individual elements of the fracture process.

Initiation and intrinsic toughness

The energy absorbed to initiate the crack corresponds to the area under the curve up to the point at which the force drops rapidly (Figure 3b) and has two components. First, the energy which is required to create the new surfaces, for which we define a corresponding intrinsic toughness G_0 . Second, the energy associated with the growth of the craze at the root of the notch. G_p denotes the calculated initiation toughness.

Side-grooved specimens were used to eliminate any contribution due to shear lips (Figures 5a and b). Figure 6 shows the results as a function of impact velocity. Values of G_p at 1 m s^{-1} are given in Table 2. No systematic variation with the volume fraction of segregated phase is observed. In fact, material A, without any segregated phase, gives the highest G_p .

Craze length (r_c) varies with impact velocity, as shown in Figure 7, smaller crazes being produced at higher velocities. By comparing the plots in Figures 6 and 7, the following observation can be made: for any given velocity, the extremes of our set of materials, i.e. A and C, exhibit different initiation toughness: $(G_p)_A > (G_p)_C$, with no difference in the associated craze length. Thus a simple correlation does not exist in this case between initiation toughness and craze length.

To calculate G_0 , a plot was constructed of G_p versus r_c . G_0 was obtained by extrapolating the data to zero craze length. The results are shown in Figure 8.

The form of the equation used to perform the extrapolation was:

$$G_p = G_0 \exp(\xi r_c) \quad (2)$$

where ξ is a constant. This equation is an empirical fit to the data but has been shown to be applicable to a variety of polyethylenes¹⁵ and gives a geometry-independent value of G_0 .

All three materials have the same G_0 , i.e. approximately 6 kJ m^{-2} . There is no effect attributable to the presence of the segregated phase. The mechanism controlling G_0 has not yet been established and requires further study, but it is worth noting that for a homopolymer of similar M_w , $G_0 \sim 2\text{--}3 \text{ kJ m}^{-2}$.

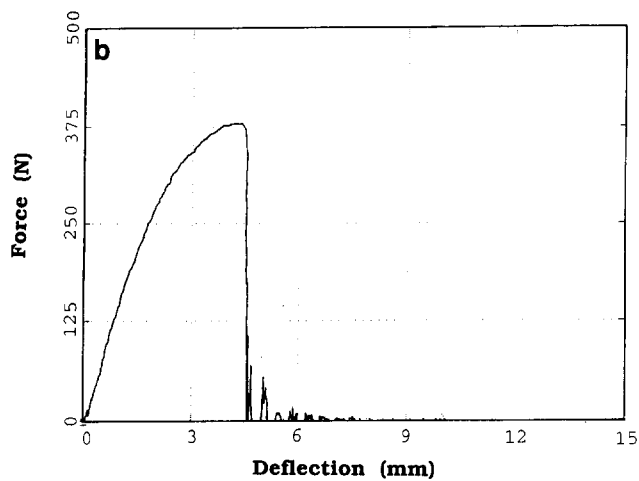
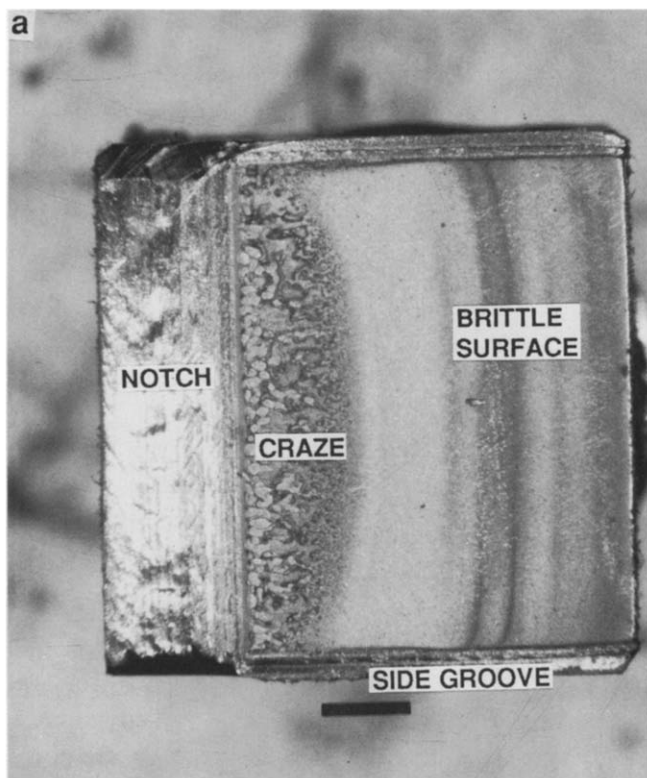


Figure 5 Determination of initiation toughness (G_p) on side-grooved rear notched specimens: (a) fracture surface (scale bar=2 mm); (b) force/deflection curve

Energy absorbed in shear lip formation

The energy absorbed in the propagation of the crack is given by the post-peak area in the curve of Figure 3b. Two energy absorbing processes are involved here, i.e. ductile failure giving rise to shear lips and the development of a hinge at the rear of the specimen. A corresponding value of the post-peak toughness (G_{pp}) can be calculated by subtracting G_p from the total toughness G_t . Values obtained at a velocity of 1 m s^{-1} are shown in Table 2. G_{pp} increases in a non-linear fashion with the concentration of segregated phase.

A separate series of experiments was carried out to establish whether the observed differences related to the extent of shear lip formation or to differences in intrinsic energy absorbing characteristics.

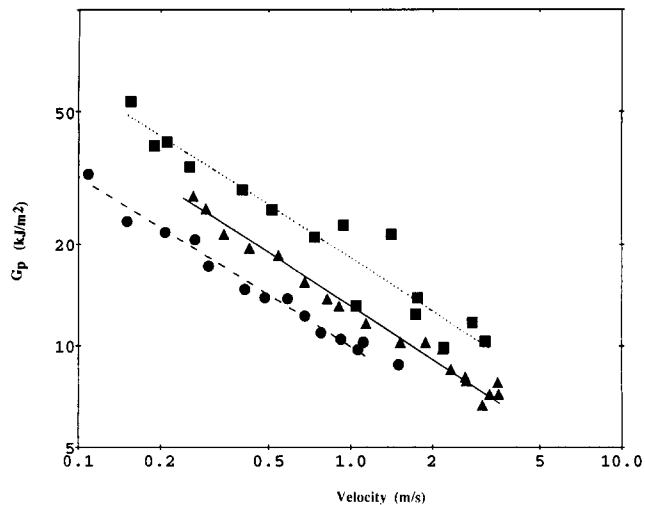


Figure 6 Initiation toughness (G_p) versus impact velocity: (■) A; (●) B; (▲) C

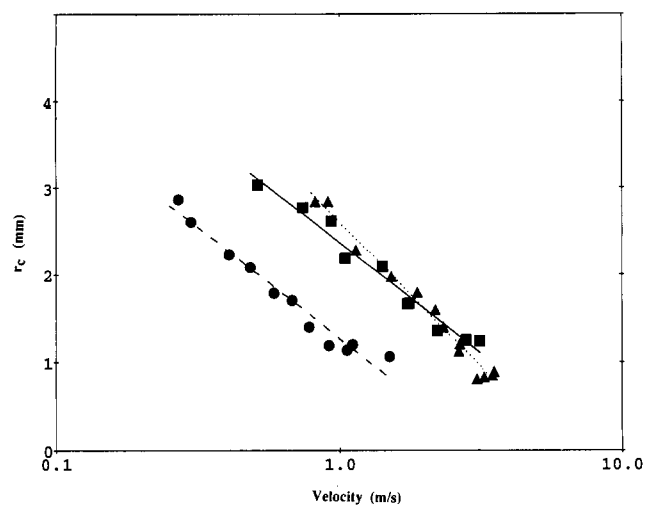


Figure 7 Craze length (r_c) versus impact velocity: (■) A; (●) B; (▲) C

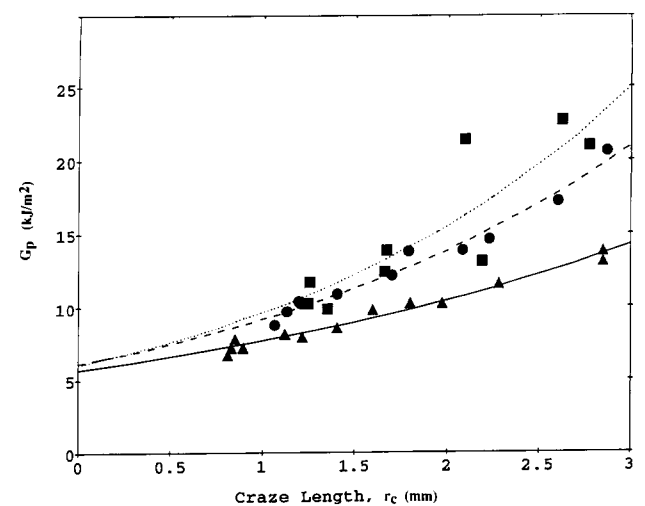


Figure 8 Initiation toughness (G_p) versus craze length (r_c): (■) A; (●) B; (▲) C

Previous work on polycarbonate¹⁶ indicated that the energy absorbed by shear lip formation is proportional to the volume of material involved. To explore this relationship in these materials the following function was used:

$$U_{SL} = kA_{SL}^{1.5} \quad (3)$$

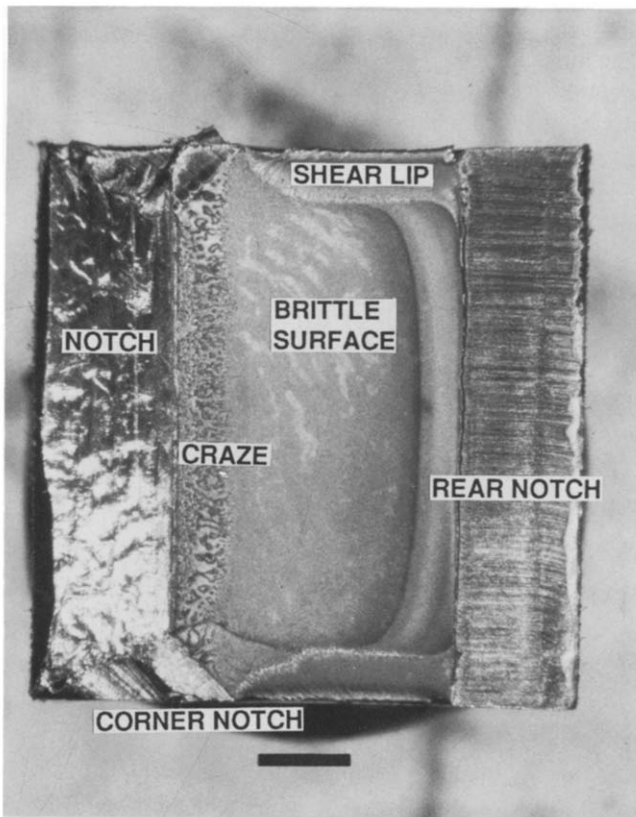


Figure 9 Fracture surface of a rear notched, side-grooved and corner notched specimen. Scale bar = 2 mm

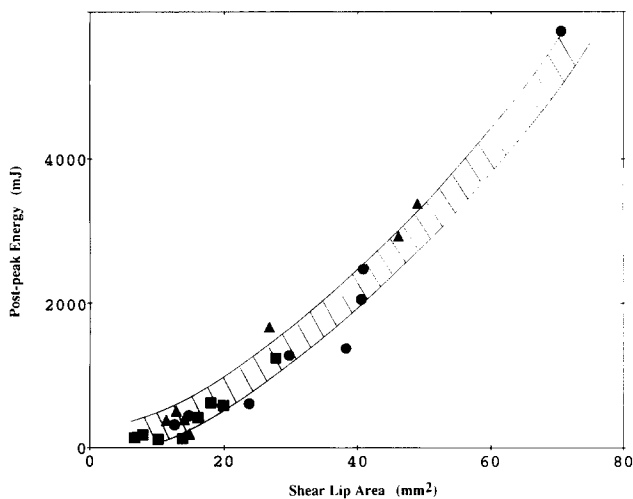


Figure 10 Post-peak energy versus shear lip area: (■) A; (●) B; (▲) C

where U_{SL} is the energy absorbed in the shear lips, and A_{SL} is the shear lip area. The constant k is proportional to the shear lip energy absorption per unit volume.

For a direct measurement of the shear lip energy, specimens with rear and corner notches were used. These notches are designed to prevent the formation of a hinge at the back of the specimen and to eliminate any interference due to the craze, respectively (Figure 9). Different specimen depths were used to vary the shear lip area. The shear lip energy for the three materials is plotted as a function of shear lip area in Figure 10. Within the experimental scatter, all the results fall on a single band which is well represented by equation (3). The implication is that there is no difference between the three

materials. Thus the different values of G_{pp} at 1 m s^{-1} (Table 2) reflect differences in the volume of material involved in shear lip formation and not differences in the specific energy absorbing characteristics of the shear lips.

DISCUSSION

The starting point for this study was the total toughness, as determined from the total energy absorbed during the Charpy test. It is important to consider what this value actually represents. At best, this may be used as a comparative measure of toughness, but with the provision that all specimens have the same test geometry. The reason for this is simply that the energy absorbing effects contributing to G_i are very geometry dependent.

The material with the highest concentration of segregated phase exhibits the highest value of G_i . The proper interpretation of this result, however, requires consideration of all the elements of the fracture event.

Intrinsic toughness for the three LLDPEs examined is the same (6 kJ m^{-2}). This is the minimum toughness in the absence of crazing and corresponds to the plane strain lower bound, G_c .

The suggestion is that, were there any toughening effect of the segregated phase then this has been suppressed. If this is the case, then there is some analogy with the toughness of rubber modified polymers at temperatures below the glass transition of the rubber. The intrinsic toughness is that determined by the polymer matrix, and so is dictated by molecular mobility over a much smaller length scale than that of the diameter of the segregated phase.

It is interesting to note that the value of 6 kJ m^{-2} is roughly twice as high as that for homopolymers of similar molecular weight⁵. The molecular mechanisms controlling intrinsic toughness in polyethylene are not yet known. The answer, however, must lie in the relaxation processes which involve molecules as well as larger morphological units, e.g. crystalline lamellae, and the way these are affected by branching. This area is ready for a fresh appraisal in the light of the present results.

In these LLDPEs, since the intrinsic toughness is the same, the observed differences in initiation toughness must reflect a difference in the crazing behaviour. Crazing of polyethylene is well documented in slow crack growth^{17,18}. Its importance in impact fracture, however, has been neglected. Recently it has been demonstrated^{10,19} that a craze zone grows during the increase in load to its peak value, and fails catastrophically at a critical point, without any slow crack growth. Furthermore the craze develops as a single entity¹⁰, with similarities to the classical crazes in polystyrene, poly(methyl methacrylate) etc., but of significantly greater thickness. Therefore, in materials where crazing occurs prior to brittle failure, it has a positive effect on initiation toughness.

A significant finding of this work is that the segregated phase has a beneficial effect on the extent of shear lip formation and consequently on the post-peak energy absorption of these materials. This is in spite of the similarity in yield stress (Table 1). The shear lips form by a bulk yielding of the material at the free surface of the specimen. Yield deformation within the shear lips is believed to be due to inter-lamellar shear²⁰, associated with the α -transition. It is suggested that the segregated phase makes inter-lamellar shear easier, having a plasticizing effect which changes the α transition.

In summary, no rubber toughening effect was found in the intrinsic fracture toughness determination, G_0 . However, a positive effect on ductile performance was discovered, but this can only be utilized where full shear lips can be developed, i.e. in sections thicker than the shear lips.

CONCLUSIONS

Two distinct factors have been identified which are responsible for the high fracture toughness of LLDPE. First, the apparently high value of the intrinsic toughness — related to the energy required to create two new surfaces. This is a fundamental material parameter which is likely to be sensitive to the structure of the polymer, e.g. to the presence or absence of short-chain branching. However, the molecular mechanisms controlling intrinsic toughness are not yet known. Second, a ductile failure phenomenon which involves extensive regions near the surface of the specimens (shear lips). The presence of a segregated 'rubbery' phase has no effect on the intrinsic toughness, but it affects the extent of shear lips formation. The higher the concentration of segregated phase, the larger the shear lips area and hence the higher the specific component of the absorbed energy.

Thus, the segregated phase contributes to the higher toughness of LLDPE, but the mechanism involved is different from a conventional rubber toughening mechanism.

ACKNOWLEDGEMENTS

The authors wish to thank BP Chemicals for permission to publish this work.

REFERENCES

- 1 Hashemi, S. and Williams, J. G. *Polymer* 1986, **27**, 384
- 2 Mai, Y. W. and Williams, J. G. *J. Mater. Sci.* 1977, **12**, 1376
- 3 Moore, D. R., Prediger, R. and Stephenson, R. C. *Plastics Rubber Process. Applic.* 1985, **5**, 335
- 4 Adams, G. C., Bender, R. G., Crouch, B. A. and Williams, J. G. *Polym. Eng. Sci.* 1990, **30**, 241
- 5 Channell, A. D. and Clutton, E. Q. *Polymer* 1992, **33**, 4108
- 6 Mirabella, F. M., Westphal, S. P., Fernando, P. L., Ford, E. A. and Williams, J. G. *J. Polym. Sci., Polym. Phys. Edn* 1988, **26**, 1995
- 7 Defoor, F., Groeninckx, G., Schouterden, P. and Van der Heijden, B. *Polymer* 1992, **33**, 3878
- 8 Wilfong, D. L. and Knight, G. W. *J. Polym. Sci., Polym. Phys. Edn* 1990, **28**, 861
- 9 Hill, M. J., Barham, P. J., Keller, A. and Rosney, C. C. A. *Polymer* 1991, **32**, 1384
- 10 Clutton, E. Q. and Channell, A. D. Proceedings of European Symposium on Impact and Dynamic Fracture of Polymers and Composites, Sardinia, September 1993
- 11 Clutton, E. Q. and Channell, A. D. in preparation
- 12 Kanig, G. *Kolloid Z. Z. Polym.* 1973, **251**, 782
- 13 Cawood, M. J. and Smith, G. A. H. *Polymer Testing* 1980, **1**, 3
- 14 Plati, E. and Williams, J. G. *Polym. Eng. Sci.* 1975, **15**, 470
- 15 Dear, J. P., Clutton, E. Q. and Channell, A. D. *Construct. Building Mater.* 1993, **7**, 207
- 16 Pitman, G. L. and Ward, I. M. *Polymer* 1979, **20**, 895
- 17 Lustiger, A. and Corneliussen, R. D. *J. Mater. Sci.* 1987, **22**, 2470
- 18 Bassani, J. L., Brown, N. and Lu, X. *Int. J. Fract.* 1988, **38**, 43
- 19 Hemingway, A. J., Channell, A. D. and Clutton, E. Q. *Plastics Rubber Comp. Process. Appl.* 1992, **17**, 147
- 20 Brooks, N. W. J. *PhD Thesis* University of Leeds, 1993